Carbohydrate Polymers 82 (2010) 472–479

Contents lists available at ScienceDirect

Carbohydrate Polymers

journal homepage: www.elsevier.com/locate/carbpol

Non-woven mats of poly(vinyl alcohol)/chitosan blends containing silver nanoparticles: Fabrication and characterization

Au Thi Hang, Beomseok Tae, Jun Seo Park*

Division of Chemical Engineering, Hankyong National University, Ansung, 456-749, Republic of Korea

ARTICLE INFO

Article history:
Received 20 January 2010
Received in revised form 6 May 2010
Accepted 7 May 2010
Available online 21 May 2010

Keywords:
Electrospinning
Chitosan
Poly(vinyl alcohol)
Polymer blend
Silver nanoparticle
Antibacterial activity

ABSTRACT

Non-woven mats of a poly(vinyl alcohol) (PVA)/chitosan (CS) blend (PVA/CS) and PVA/CS blends incorporated with silver (Ag) nanoparticles (Ag/PVA/CS) were fabricated by an electrospinning method. The electrospun fibers attained a beaded structure at PVA to CS weight ratios of up to 88/12. The addition of $AgNO_3$ to the PVA/CS blend solution improved the electrospinnability. The morphology of the electrospun non-woven mats was observed by Field Emission Scanning Electron Microscopy. The formation of Ag nanoparticles on the surface of the electrospun fibers was confirmed by Transmission Electron Microscopy and by obtaining X-Ray Diffraction Spectra. The thermal properties of the polymer blends and the effect of the Ag nanoparticles on the crystallization of the polymer blends were examined by Differential Scanning Calorimetry. The mechanical properties of the PVA/CS blend non-woven mats were evaluated by tensile testing. Higher antibacterial activity was observed in the non-woven mats of Ag/PVA/CS blends than in those of PVA/CS blends.

1. Introduction

Electrospinning is a process used to fabricate submicron fibers using an electrically charged jet of diverse materials, including polymers with diameters ranging from several micrometers to several hundreds of nanometers. Because electrospun (e-spun) nanofibers have high porosity and a very small pore size, they have a larger specific surface area than a cast film (Jia et al., 2007). Non-woven mats made of such e-spun fibers show great potential for a variety of applications, especially biomedical applications such as wound dressings, drug delivery systems, and antibacterial applications (Pillai, Paul, & Sharma, 2009; Zhou, Yang, & Niel, 2006).

Chitosan (CS), a (1-4)-linked-2-amino-2-deoxy-β-D-glucopyranose, is one of the most abundant natural polysaccharides and has been widely studied because it has many useful properties: it is non-toxic, biodegradable, biocompatible, bioactive, and has antibacterial properties (Giner, Ocio, & Lagaron, 2008; Jia et al., 2007; Zhou et al., 2006). One of the most useful properties of CS is its antibacterial activity, which is beneficial in wound dressings, drug delivery systems, antimicrobial applications, membrane filtration, and various tissue-engineering applications (Jameela & Jayakrishnan, 1995; Khoo, Franzich, Rosinski, Sjostrom, & Hoogstraate, 2003; Muzarelli, 2009; Shalumon et al., 2009). However, CS cannot be directly fabricated by the electrospinning process because of its polycationic nature in solution (Giner, Ocio, & Lagaron, 2009; Park, Leong, Yoo, & Huson, 2004). To overcome this shortcoming of CS, many researchers have sought to improve its electrospinning ability by mixing CS with other polymers such as poly(vinyl pyrrolidone) (PVP), poly(ethylene oxide) (PEO), silk fibroin (SF), and zein (An, Zhang, Zhang, Zhao, & Yuan, 2009; Giner et al., 2009; Ignatova, Manolova, & Rashkov, 2007; Park et al., 2004).

Poly(vinyl alcohol) (PVA) and CS blends have been fabricated successfully by the electrospinning process (Jia et al., 2007; Zheng, Du, Yu, Huang, & Zhang, 2001; Zhou et al., 2006). PVA has many useful properties such as biocompatibility, biodegradability, and good mechanical properties (Ding, Kim, Lee, Lee, & Choi, 2002; Jin, Yang, Zhou, Ma, & Nie, 2008). Moreover, PVA has an inherent fiber- and film-forming ability, which facilitates easy fiber production (Ignatova, Starbova, Markova, Manolova, & Rashkov, 2006). CS can be blended with PVA for electrospinning since CS and PVA are partially miscible and have similar characteristics during the electrospinning process; for example, they become coagulated, oriented, and cross-linked (Zheng et al., 2001). A blend of PVA and CS not only has the characteristics of each component, but also has other useful properties, such as good electrospinnability and mechanical properties, that make it a possible candidate material for use in antimicrobial applications (Chuanchamsai, Lertviriyasawat, & Danwanichakul, 2008).

It has been proposed that adding a small amount of salt to the polymer solution could improve the electrospinning ability since the salt contributes to the change in the morphology of the e-spun

* Corresponding author. Tel.: +82 31 670 5202; fax: +82 31 675 9604.
E-mail address: jspark@hknu.ac.kr (J.S. Park).

0144-8617/$ – see front matter © 2010 Elsevier Ltd. All rights reserved.
doi:10.1016/j.carbpol.2010.05.016

fibers from a bead-on-fiber structure to a uniform fiber structure (Zong et al., 2002). When $AgNO_3$ is added to a PVA/CS blend solution, Ag^+ is reduced to Ag^0 during the electrospinning process or by heat treatment. In addition, CS is able to react with $AgNO_3$ by chelation, causing a decrease in the repulsive forces between ionic groups within polymer backbones (An et al., 2009; Jin, Jeon, Kim, & Youk, 2007; Park et al., 2004; Velmurugan, Kumar, Han, Nahm, & Lee, 2009; Wei, Sun, Qian, Ye, & Ma, 2009). Therefore, a continuous fiber can be e-spun from Ag^+/PVA/CS solutions with high concentrations of CS. Moreover, silver (Ag) nanoparticles and Ag ions are known to have higher antibacterial ability than other metals (Jin et al., 2007; Velmurugan et al., 2009). The antibacterial activity of CS incorporated with Ag (silver ions or nanoparticles) is higher than that of each component (Wei et al., 2009). Thus, $AgNO_3$ added to PVA/CS blend solutions can improve their electrospinning ability and antibacterial activity.

To gain a better understanding of the electrospinning process parameters, we investigated the viscosity, ionic conductivity, and CS content of polymer blend solutions. $AgNO_3$ was added to PVA/CS blend polymer solutions to enhance not only the electrospinning performance but also the antibacterial ability of non-woven mats of PVA/CS. The microstructures of non-woven mats of PVA/CS blends and Ag/PVA/CS blends were examined by Field Emission Scanning Electron Microscopy (FE-SEM). The formation of Ag nanoparticles on the surface of the e-spun fibers in the non-woven mats, and their average size and shape, were determined by Transmission Electron Microscopy (TEM) and by obtaining X-ray Diffraction Spectra (XRD). Thermal analysis was carried out by Differential Scanning Calorimetry (DSC) to study the thermal properties of PVA/CS blends and Ag/PVA/CS blends, as well as the effect of Ag nanoparticles on the cold crystallization of e-spun fibers. The mechanical properties of the non-woven mats were measured by tensile tests. The antibacterial activity of the non-woven mats was examined using the viable cell-counting method.

2. Experimental

2.1. Materials

CS (Mv 690,000, degree of deacetylation 90%) was obtained from the Bio Materials Co. (Korea). PVA (Mw 98,000, degree of hydrolysis 88%) was purchased from Acros Organics (USA). Acetic acid (99.55%) and silver nitrate ($AgNO_3$) were purchased from the Samchun Chemical Co. (Korea). Glutaraldehyde solution (40%) was purchased from Aldrich (USA). Double-distilled water was used.

2.2. Measurement of viscosity and ionic conductivity

The ionic conductivity of the PVA/CS blend solutions was determined using a conductivity meter (HI 2300, Hanna Instruments, Korea) under ambient atmosphere. The viscosity of each solution was measured using a viscometer (LVDVII, Brookfield, USA). The solution was first placed into the viscometer chamber and then into a water jacket. Viscosity measurements were conducted using a #18 cylindrical spindle under ambient atmosphere.

2.3. Electrospinning

PVA was expanded in ethanol and dissolved completely in water at a concentration of 12 wt%. CS powder was dissolved in an acetic acid/water solution (2 wt%) at a concentration of 4 wt%. The CS solution was mixed with the PVA solution at various weight ratios (PVA/CS): 100/0, 96/4, 92/8, 88/12, 82/18, and 75/25. Silver nitrate (1 wt%) was added to the PVA solution to obtain an $AgNO_3$/PVA solution. The CS solution was also mixed with the $AgNO_3$/PVA solution at various weight ratios (PVA/CS): 100/0, 96/4, 92/8, 88/12, 82/18, and 75/25 to prepare polymer solutions (Ag^+/PVA/CS) for the electrospinning. Electrospinning was performed at room temperature with a voltage of 12 kV and a tip-to-collector distance of 14.5 cm. The rate of spinning ranged from 2 μl/min to 3.5 μl/min. Each of the prepared solutions was stored in a standard 5-ml plastic syringe that was attached to a blunt 22-gauge stainless steel hypodermic needle. The solution flow rate was controlled by a syringe pump. A high supply voltage was connected to the hypodermic needle, which was used as a positive electrode.

2.4. Heating–annealing

The non-woven mats of PVA/CS blends containing silver (Ag^+ ion, Ag nanoparticles) were heated at 130 °C for 16 h in an oven.

2.5. Cross-linking of non-woven mats

The non-woven PVA/CS blend and Ag/PVA/CS blend mats were immersed in a 1.25 wt% glutaraldehyde (GA)/acetone mixture at room temperature for 6 h. After cross-linking, the non-woven mats were purified by copious amounts of an acetone/water solution and dried at 60 °C under vacuum for 24 h.

2.6. Instrumentations

The morphology of the non-woven mats was observed by FE-SEM using a HITACHI S-4700 (Japan) with a BAL-TEC MED_020 coating system. A Tecnai_G2 TEM was used to observe Ag nanoparticles on the surface of the e-spun fibers in the non-woven mats with carbon-coated copper grids.

XRD patterns of the e-spun fibers were recorded with a Rigaku Dmax-II X-ray diffractometer (Rigaku USA), using Nickel-filtered Cu K_α radiation at 40 kV and 50 mA in the diffraction angle range $2\theta = 5–80^\circ$.

The thermal behavior of non-woven mats of PVA/CS blends was checked by DSC (TA Instruments, USA). The melt behavior of the non-woven mats was examined by heating at 10 °C/min in a nitrogen flow. The cold crystallization behavior was investigated by first keeping the samples at 280 °C for 5 min to remove the thermal history and then cooling the samples at a cooling rate of 10 °C/min to room temperature.

The mechanical properties of the PVA/CS non-woven mats were determined using a Lloyd testing machine (Lloyd Instruments, UK). The non-woven mats were tested with a 0.1 N preload at a cross-head speed of 5 mm/min. The length, width, and thickness of test sheets of the non-woven mats were about 30 mm, 10 mm, and 50 μm, respectively. The average values from five repetitions were taken as the tensile strength and elongation at break results.

2.7. Antibacterial testing

The antibacterial activity of the non-woven mats was tested using *Escherichia coli* (*E. coli*) bacteria. *E. coli* (0.1 ml) was cultivated in 100 ml of a Difco Nutrient Broth solution, to give a bacterial concentration of about 7×10^{11} CFU/ml. After this, 1 ml of the bacteria/nutrient solution was added to 9 ml of sterilized Difco Nutrient Broth solution (0.8%). Several decimal dilutions were performed until the bacterial concentration went from 7×10^3 to 7×10^7 CFU/ml. For the antibacterial testing, non-woven mats of PVA/CS blends and Ag/PVA/CS blends were put into the solution and then incubated and shaken at 37 °C for 15 h. The weight and size of the non-woven mats of PVA/CS or Ag/PVA/CS were 18 mg and 50 μm × 4 cm × 3 cm, respectively. After the incubation, 0.1 ml of the solution was taken out and quickly spread on a plate containing nutrient agar. Plates containing bacteria were incubated at

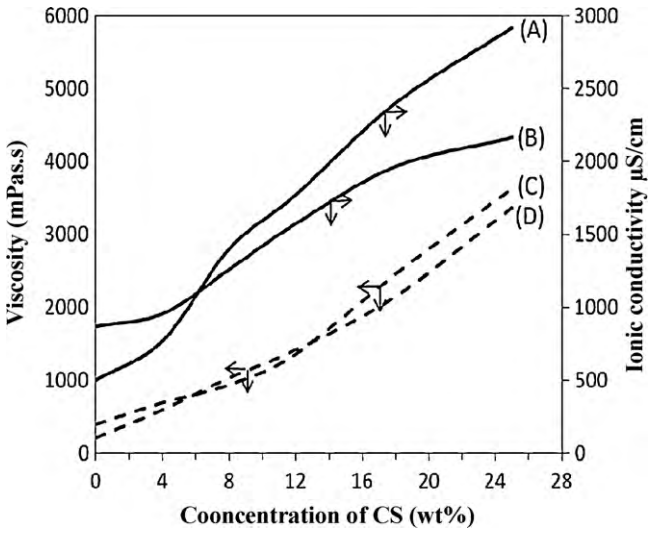

Fig. 1. Effect of the ionic conductivity of PVA/CS blend (A) and Ag^+/PVA/CS blend (B), and viscosity of PVA/CS blend (C) and Ag^+/PVA/CS blend (D) with different weight ratios of PVA and CS in the polymer blend solutions. All measurements were conducted at room temperature.

37 °C for 24 h, and then the numbers of the surviving colonies were counted.

2.8. Bactericidal kinetic testing

Non-woven mats of PVA/CS blend and Ag/PVA/CS blend were added to tubes containing the test bacteria at a concentration of 7×10^6 CFU/ml in the Difco Nutrient Broth solution. The tubes were kept in an incubated shaker at 37 °C. Samples of non-woven mats of PVA/CS and Ag/PVA/CS blends with the same weight and size (18 mg and 50 μm × 4cm × 3 cm), as mentioned, were also used. 0.1 ml of the solution was taken out and quickly spread on a plate containing nutrient agar every hour. The plates containing bacteria were incubated at 37 °C for 24 h and the bacterial colonies were counted.

3. Results and discussion

3.1. Morphology of non-woven mats of PVA/CS blends and Ag/PVA/CS blends

The performance and morphology of the e-spun fiber mats were affected by many factors, including the physicochemical properties of the polymer solution and the electrospinning process parameters. The viscosity and ionic conductivity of polymer solutions are considered to be major parameters in electrospinning (Jia et al., 2007; Zhou et al., 2006). In the present study, measurements were performed on the viscosity and ionic conductivity of the PVA/CS blend solutions with and without the addition of $AgNO_3$ at various concentrations of CS in the polymer solutions.

Lines A and B in Fig. 1 show the effect of the CS content on the ionic conductivity of the PVA/CS and Ag^+/PVA/CS blend solutions, respectively. It was found that the ionic conductivity of the polymer solutions increased with the increase of CS content (as shown in line A), due to an increase in the $-NH_3^+$ groups of the CS. This occurred because, when the CS was dissolved in the acetic acid solution, the $-NH_2$ of the CS became $-NH_3^+$. The same trend was observed for the case of the Ag^+/PVA/CS blend solution, as shown in line B. When the amount of CS in the polymer solution was less than 6 wt%, the ionic conductivity of the Ag^+/PVA/CS polymer solution was higher than that of the PVA/CS blend solution with the same weight ratio of PVA to CS in the blend. However, when the concentration of CS was higher than 6 wt%, the ionic conductivity of the Ag^+/PVA/CS solution was lower than that of the PVA/CS solution with the same CS content. This is attributed to the Ag^+ of the Ag^+/PVA/CS solutions, which inhibited the ionizability of the amino group of the CS by a chelating mechanism.

Lines C and D in Fig. 1 present the effect of the CS content and the presence of Ag^+ in the polymer solution on the viscosity of polymer solutions of the PVA/CS blend and Ag^+/PVA/CS blend, respectively. The increase in the viscosity of a polymer solution with an increase in the CS content was due to the high viscosity of the CS and to the effect of the intermolecular interactions between the PVA and CS, such as hydrogen bonding in the solution state (Jia et al., 2007). However, as can be seen in line D, the effect of the $AgNO_3$ on the viscosity of the polymer solutions was not pronounced.

Fig. 2 shows FE-SEM micrographs, average diameter, and diameter distribution of the non-woven mats made of the PVA/CS blend e-spun fibers at different weight ratios of PVA to CS under a 12 kV process condition. As shown in Figs. 2(a)–(c), a good fibrous structure was observed for the non-woven mats with PVA to CS weight ratios up to 92/8. The e-spun fibers in the non-woven mats became beaded at PVA to CS weight ratios ranging from 88/12 to 75/25, as can be seen in Fig. 2(d)–(f). When the CS content in the PVA/CS blend was higher than 12 wt%, e-spun fibers could hardly be formed. This behavior can be explained as: when the concentration of the CS (a polycationic polymer) in the blend solution increased, the repulsive force between the ionic groups within the polymer's backbone increased. Thus, the formation of continuous fibers was inhibited during the electrospinning process under a high electric field. Simultaneously, as the concentration of CS in the blend increased from 0 to 25 wt%, the average diameters of PVA/CS blend e-spun fibers decreased from 533.9 nm to 114.2 nm, and the diameter distribution become slightly narrower. Since, the increasing CS contents in the polymer solutions led to the increased charge density on the surface of the ejected jet formed during electrospinning (Son, Youk, Lee, & Park, 2004).

Fig. 3 shows FE-SEM micrographs of the non-woven mats of the PVA/CS blends containing $AgNO_3$ with different PVA to CS weight ratios; their average diameter; and their diameter distribution, e-spun at the voltage of 12 kV. The average diameter of the e-spun fibers in a PVA non-woven mat containing silver was around 577.1 nm, which was quite similar to that of the PVA non-woven mat which had no silver, indicating that the presence of $AgNO_3$ in the polymer solution did not affect the size of the e-spun fibers. From the comparison of results between Figs. 3 and 2, the diameters of the e-spun fibers of the non-woven mats in Fig. 3 also tended to decrease when the CS content in the polymer blend solutions increased. No bead formation was observed in the non-woven mats of the Ag^+/PVA/CS blends at PVA to CS weight ratios of 88/12, 82/18, and 75/25, as shown in Fig. 3(d)–(f). The microstructure of these non-woven mats was different from that of the PVA/CS mats shown in Fig. 2(d)–(f). Since there was not much difference in viscosity between the PVA/CS and Ag^+/PVA/CS blend solutions, the difference in the ion conductivities of these blend solutions was responsible for the difference in the morphologies of the non-woven mats of the PVA/CS blends and those of the Ag^+/PVA/CS blends. The addition of $AgNO_3$ salt to the polymer blend solutions caused coordinate interactions between the NH_2 groups of the CS and the Ag ions, which decreased the repulsive forces between the ionic groups within the polymer backbone of the CS and made it possible to perform stable electrospinning under a high electric field (Park et al., 2004; Velmurugan et al., 2009; An et al., 2009; Wei et al., 2009). Hence, the addition of $AgNO_3$ to a PVA/CS solution improved the electrospinning ability of PVA/CS blend solutions. The morphology of the e-spun fibers of Ag/PVA/CS became "no bead" and "uniform fiber structure" at high CS content in the polymer blend solution.

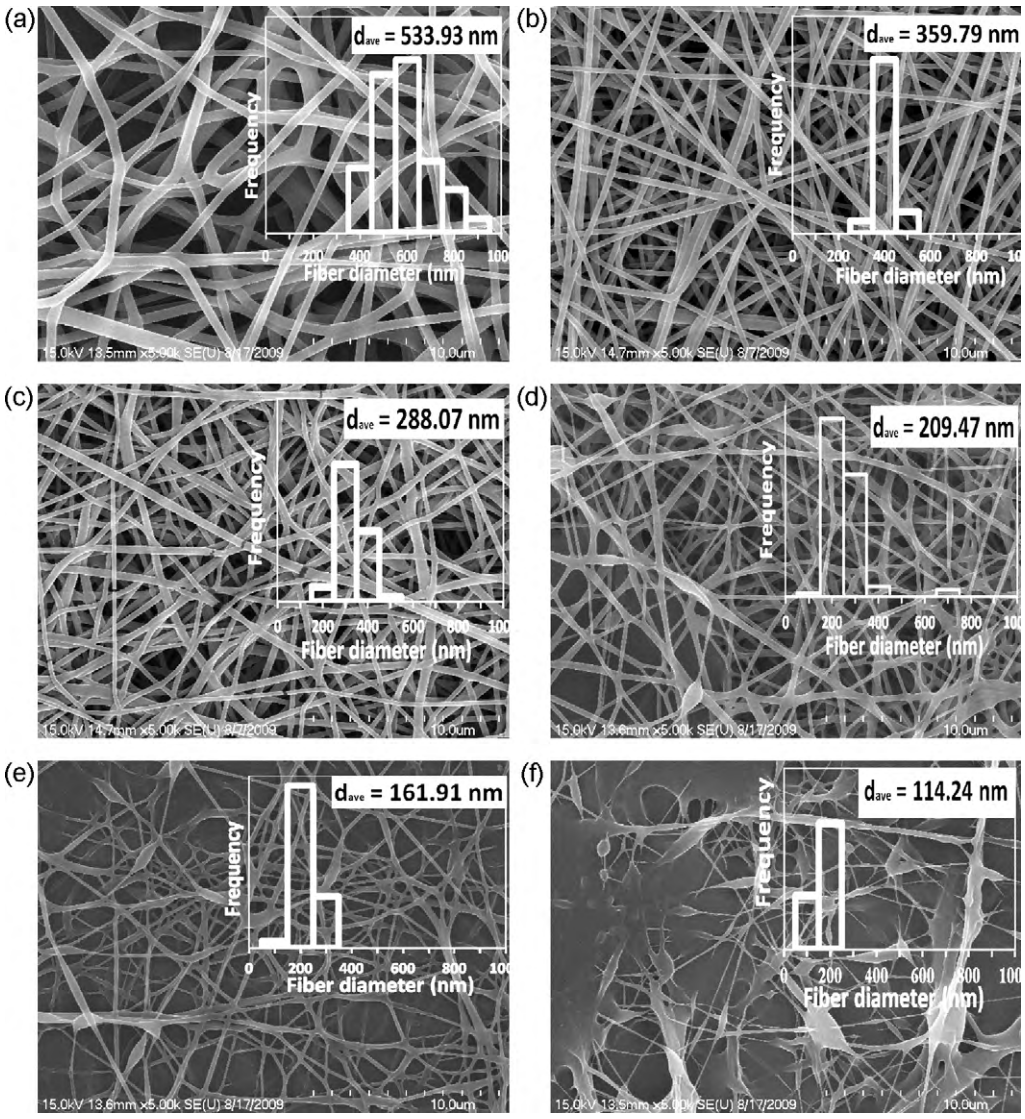

Fig. 2. FE-SEM micrographs, average diameter (d_{ave}) and diameter distribution of PVA/CS non-woven mats with different PVA to CS weight ratios: (a) 100/0, (b) 96/4, (c) 92/8, (d) 88/12, (e) 82/18, and (f) 75/25. The electrospinning was conducted under the process conditions of a voltage of 12 kV, distance of 14.5 cm, and flow rate of 3.5 μl/min.

Fig. 4 shows TEM micrographs of the fibers that were e-spun from the polymer solution of Ag^+/PVA/CS blends with different PVA to CS weight ratios. Ag nanoparticles can be observed on the surface of e-spun fibers of the PVA/CS blends. Ag nanoparticles were spontaneously generated from the Ag^+ ion in PVA polymer solutions during the electrospinning process (Jin et al., 2007). PVA nanofibers containing Ag nanoparticles were also produced by heat treatment of the e-spun nanofiber mats at various temperatures and times (Hong, Park, Sul, Youk, & Kang, 2006; Jin et al., 2007). In the Ag/PVA/CS blend solution, Ag nanoparticles were formed not only by the heat treatment of Ag^+ ion in this polymer solution, but also by the reaction between chitosan and silver nitrate at high temperature (An et al., 2009; Velmurugan et al., 2009; Wei et al., 2009). In this study, all of the non-woven mats of Ag/PVA/CS blends were heat-annealed at 130 °C for 16 h in an oven. The average diameters and the size distributions of the Ag nanoparticles on the surface of e-spun fibers are shown in each TEM micrograph in Fig. 4. The average sizes of the Ag nanoparticles were 2.44 nm, 6.05 nm, 6.78 nm, and 10.74 nm depending on the content of CS in the PVA/CS blends: (a) 0%, (b) 4%, (c) 5.5%, and (d) 12%, respectively. It is observed from Fig. 4 that the size of the Ag nanoparticles increased but the number of the particles decreased with the increase of the CS content in the blends. This can be explained by the fact that adding $AgNO_3$ to a PVA/CS blend solution allows the amino and hydroxyl groups of the CS to interact with the Ag^+ by chelating (Velmurugan et al., 2009; Wei et al., 2009); hence, the CS can enclose the Ag nanoparticles and combine them. This makes the number of Ag nanoparticles on e-spun fiber surfaces decrease and the size of the Ag nanoparticles increase.

3.2. XRD analysis

XRD was used to confirm the formation of Ag nanoparticles. Fig. 5 shows the XRD patterns of Ag/PVA/CS (A) and PVA/CS (B). The strong reflection around 28.3° was attributed to crystalloid of CS, while those at 14.2° and 19.5° were assigned to crystalline PVA (An et al., 2009; Jia et al., 2007). The characteristic peak at 2θ of 38.1°, as shown in Fig. 5, confirms that the Ag nanoparticles are formed on the surface of the PVA/CS non-woven mats, since this peak is one of the characteristics of Ag nanoparticles formation (An et al., 2009; Kim, Kim, & Lee, 2010; Velmurugan et al., 2009). Thus, the XRD results given in Fig. 5 can confirm that Ag nanoparticles formed on the surface of the present fabricated PVA/CS nanofibers. The formation of Ag nanoparticles on the surface of e-spun fibers

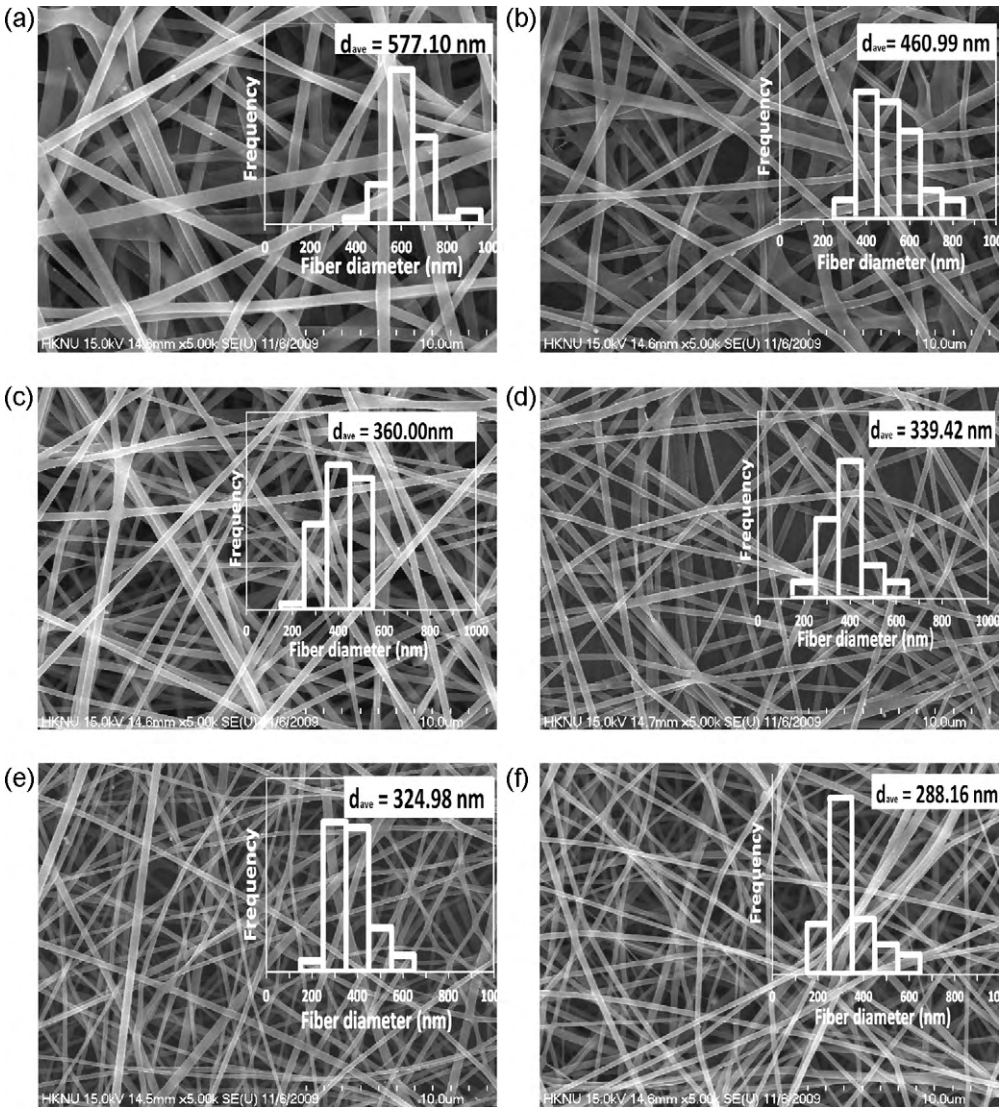

Fig. 3. FE-SEM micrographs, average diameter (d_{ave}) and diameter distribution of Ag/PVA/CS non-woven mats with different PVA to CS weight ratios: (a) 100/0, (b) 96/4, (c) 92/8, (d) 88/12, (e) 82/18, and (f) 75/25. The electrospinning was performed under the process conditions of a voltage of 12 kV, distance of 14.5 cm, and flow rate of 3.5 μl/min.

studied in this work can also be observed in the TEM micrographs given in Fig. 4.

3.3. Thermal analysis, DSC

Fig. 6(a) shows DSC thermograms of non-woven mats of PVA/CS blends with different PVA to CS weight ratios. All of the PVA/CS blend non-woven mats showed an endothermic curve with a peak at about 197 °C. When the CS content increased, the endothermic curve of a PVA/CS blend non-woven mat became broader and obtuse. The melting point and endothermic heat (ΔH_m) in the DSC thermogram curves decreased with an increase in the CS content in the blend. The melting point depression of the PVA in the blends indicates that there was some partial miscibility between the PVA and CS in the blends, confirming a previous experiment (Park, Park, & Ruckenstein, 2001). The decrease in the endothermic heat is attributed to some destruction of the crystalline structure of the PVA in the polymer blends by the presence of amorphous CS with its dilution effect.

Fig. 6(b) shows the cold crystallization curves of non-woven mats of PVA/CS blends and Ag/PVA/CS blends. It was found that the crystallization temperatures of the Ag/PVA and Ag/PVA/CS non-woven mats were higher than those of PVA and PVA/CS, indicating that the crystallization of a non-woven mats of a PVA/CS blend containing Ag (Ag/PVA/CS) took place at a higher temperature than that of a non-woven mats of the PVA/CS blends. This indicates that the Ag nanoparticles in the e-spun fibers acted as a nucleating agent. When the crystallization temperature of PVA (as shown in (B)) is compared with that of the PVA/CS (as shown in (D)), the exothermic peak area of (B) is larger than that of (D). The exothermic heat of crystallization of the polymer blend decreases with the inclusion of CS in the polymer blend. The amorphous CS in the PVA/CS blends retarded the movement of the main chain of PVA, delaying the initiation of crystallization and resulting in a less ordered structure for the crystalline PVA in the PVA/CS polymer blends. Results of DSC analysis indicate that the ordered association of PVA molecules is strongly constrained by the CS content in the PVA/CS polymer blend (Jia et al., 2007; Park et al., 2001).

3.4. Tensile tests

The mechanical strength of the non-woven mats of various PVA/CS blends was measured. Fig. 7 shows the test results of stress and elongation at break of the non-woven mats of PVA/CS blends with different PVA to CS weight ratios in the blend: (A) 100/0, (B) 96/4, (C) 92/8, and (D) 88/12, respectively. It is known that CS has

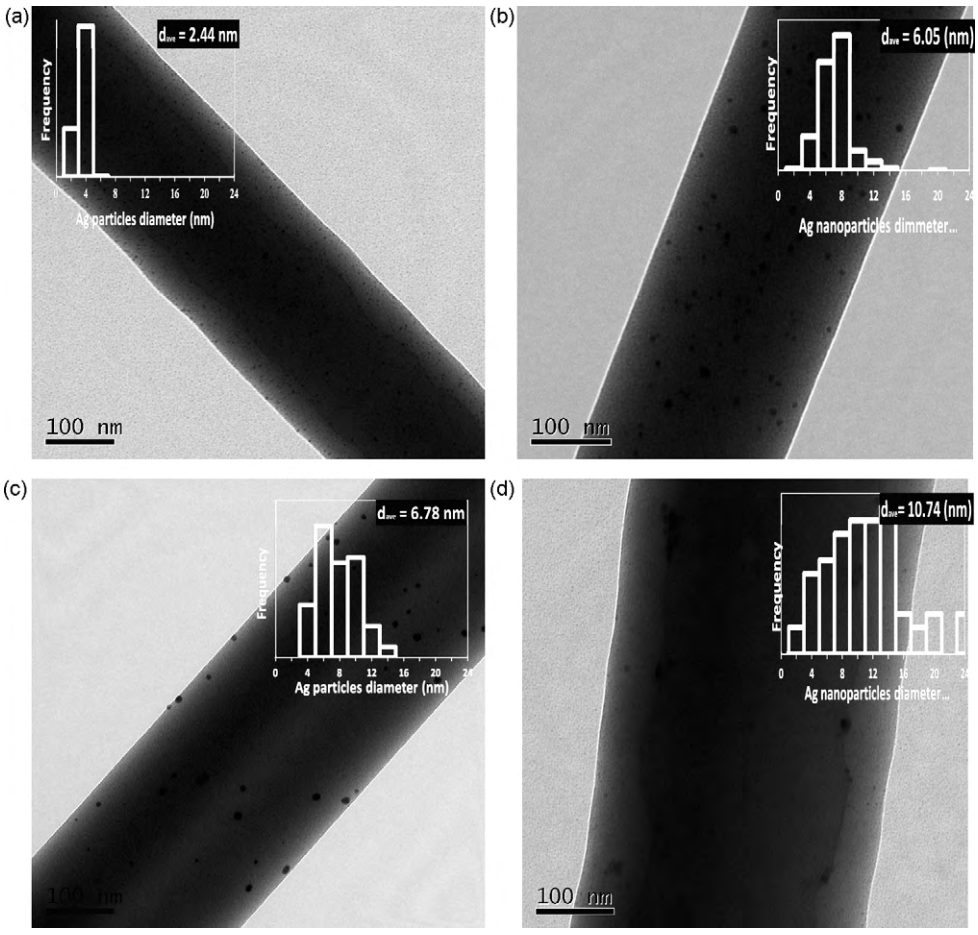

Fig. 4. TEM micrographs of e-spun fibers of Ag/PVA/CS blends with various amounts of CS (wt%) in the polymer blend: (a) 0, (b) 4, (c) 5.5, and (d) 12.

amino groups and hydroxyl groups in the backbone and is a rigid and brittle natural polymer (Park et al., 2004). From Fig. 7 it was found that when the concentration of CS in the non-woven mats of PVA/CS blends increased, the tensile strength at break of the non-woven mats also increased, while the elongation at break of the non-woven mats decreased. The results of the mechanical properties testing of the non-woven mats are thus proof of the existence of some partial miscibility between the PVA and CS in the polymer blends.

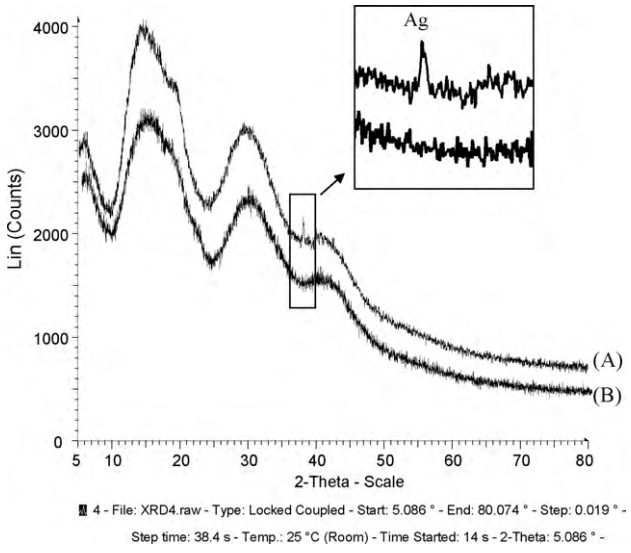

Fig. 5. XRD patterns of the non-woven mat of Ag/PVA/CS (A) and the non-woven mat of PVA/CS (B); the PVA/CS weight ratio was 96/4.

3.5. Antibacterial tests

The antibacterial activity of chitosan is based on the damaging interaction of polycations with the negatively charged surfaces of bacteria, resulting in loss of membrane permeability, cell leakage, and cell death (Ignatova et al., 2006). The antibacterial activity of the non-woven mats of the PVA/CS and Ag/PVA/CS blends against *E. coli* were tested using the viable cell-counting method. The effects of the non-woven mats on the growth of the recombinant bacteria *E. coli* are shown in Fig. 8.

Fig. 8(a) shows the antibacterial activity of the non-woven mats of various PVA/CS blends and different concentrations of bacteria. As shown in plates D_2, C_3, and B_4 in Fig. 8(a), bacteria colonies were not observed. This suggests that non-woven mats of the PVA/CS blends with weight ratios of 96/4, 92/8, and 88/12 could kill the bacteria at concentrations of 7×10^4, 7×10^5, and 7×10^6 CFU/ml, respectively. Moreover, at the same concentrations of bacteria, the antibacterial ability of the non-woven mats of PVA/CS blends increased with increase of the CS content in the blends (see Fig. 8(a)). This behavior demonstrates the antibacterial activity of the CS in the non-woven PVA/CS blend mats.

The antibacterial activity of the non-woven mats of PVA/CS containing Ag nanoparticles (Ag/PVA/CS mats) was also studied

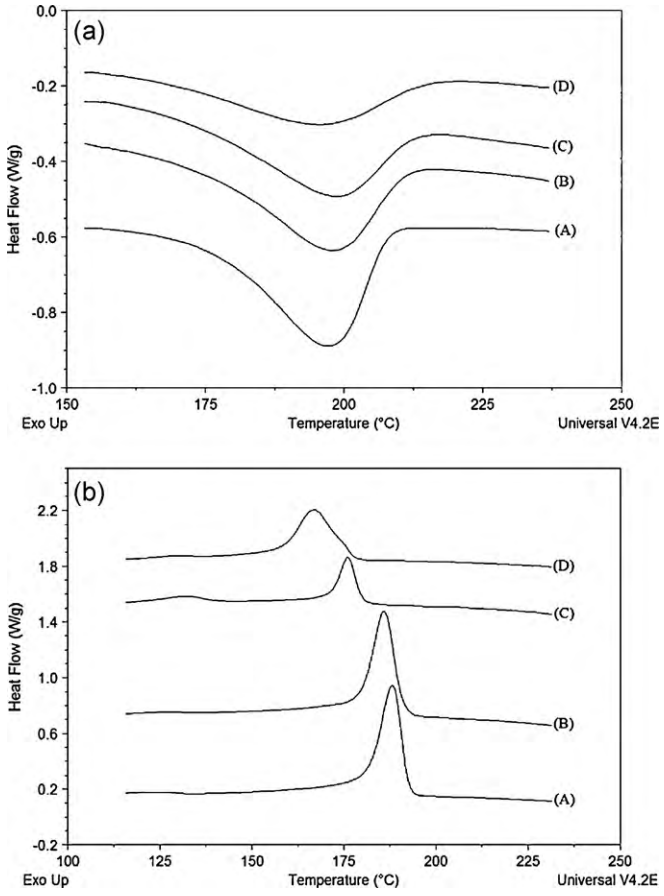

Fig. 6. (a) DSC thermograms of non-woven mats of PVA/CS blends with different PVA/CS weight ratios of (A) 100/0, (B) 96/4, (C) 92/8, and (D) 88/12. The rate of heating was 10 °C/min in a nitrogen flow. (b) DSC thermograms of PVA/CS blends and Ag/PVA/CS blends: (A) Ag/PVA non-woven mat, (B) PVA non-woven mat, (C) Ag/PVA/CS non-woven mat with a PVA/CS weight ratio of 88/12, and (D) PVA/CS non-woven mat with a PVA/CS weight ratio of 88/12. The rate of cooling was 10 °C/min in a nitrogen flow. Before cooling, the samples were kept for 5 min at 280 °C in a nitrogen flow.

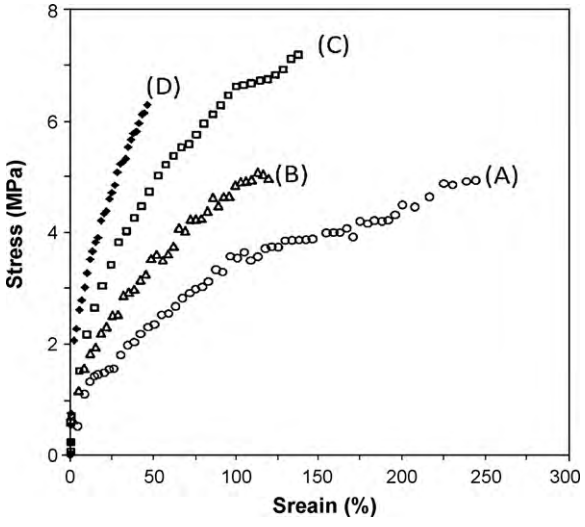

Fig. 7. Stress–strain curves of PVA/CS blend non-woven mats with various CS contents (wt%): (A) 0, (B) 4, (C) 8, and (D) 12. The non-woven mats were tested with a 0.1 N preload at a cross-head speed of 5 mm/min. The length, width and thickness of the non-woven mat were about 30 mm, 10 mm and 50 μm, respectively.

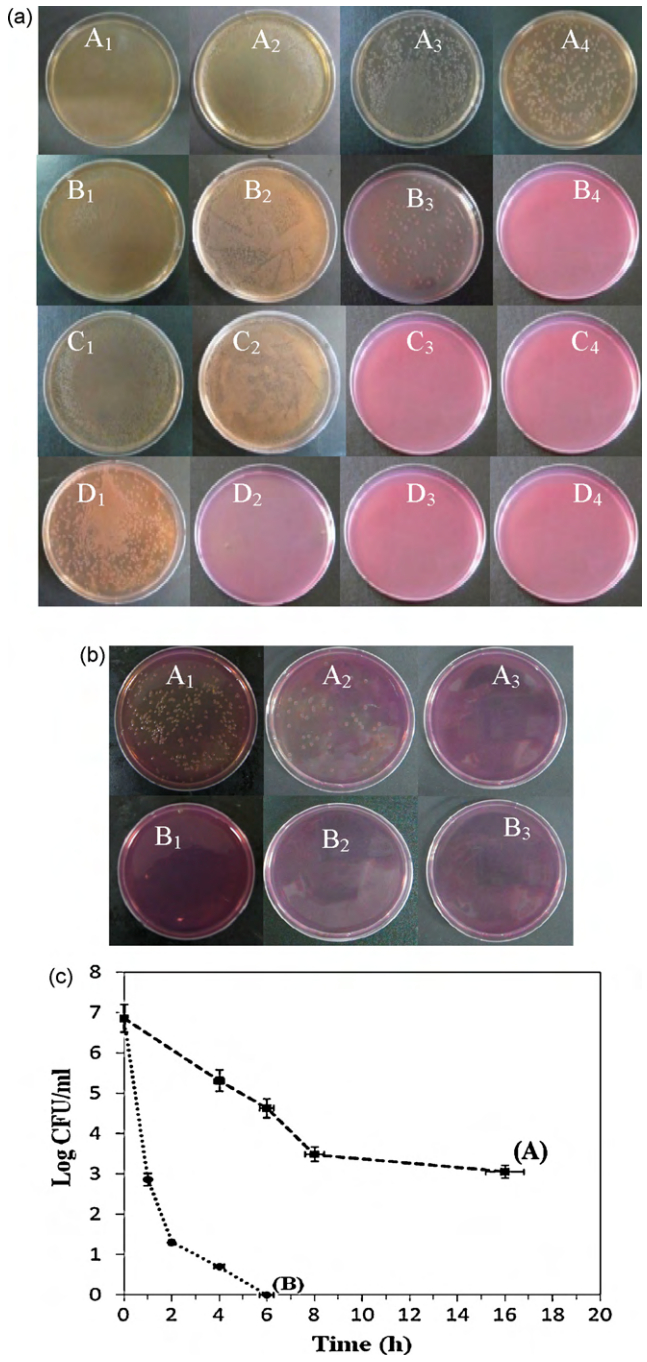

Fig. 8. (a) Antibacterial tests of the non-woven mats of PVA/CS blends with different PVA to CS weight ratios; the subscripts begin from the left-hand to right-hand side: (1): 100/0, (2): 96/4, (3): 92/8, (4): 88/12, respectively. From upper to lower the concentration of bacteria is lower; (A) 7×10^7 CFU/ml, (B) 7×10^6 CFU/ml, (C) 7×10^5 CFU/ml, and (D) 7×10^4 CFU/ml, respectively. (b) Antibacterial tests of the non-woven mats of Ag/PVA/CS with different PVA to CS weight ratios; the subscripts begin from the left-hand to right-hand side; (1): 100/0, (2): 96/4, (3): 88/12. (A): 7×10^7 CFU/ml and (B): 7×10^6 CFU/ml. The non-woven mats were put in solution and then incubated and shaken at 37 °C for 15 h. The weight and size of the non-woven mat of PVA/CS blend or Ag/PVA/CS blend were 18 mg and 50 μm × 4cm × 3 cm, respectively. After the incubation, 0.1 ml of the solution were taken out and quickly spread on a plate containing nutrient agar. Then the plates containing bacteria were incubated at 37 °C for 24 h. (c) Kinetics of the antibacterial activity of the non-woven mats of Ag/PVA/CS blend (A) and PVA/CS blend (B) toward *E. coli*; the PVA/CS weight ratio was 92/8. The bacteria concentration was 7×10^6 CFU/ml. The weight and size of the non-woven mats of PVA/CS blend or Ag/PVA/CS blend were 18 mg and 50 μm × 4cm × 3 cm, respectively. The non-woven mats were put in the bacterial solution and then incubated. 0.1 ml of the solution was taken out and quickly spread on a plate containing nutrient agar every hour. Then the plates containing bacteria were incubated at 37 °C for 24 h.

to compare to that of PVA/CS mats. Fig. 8(b) shows the antibacterial activity of the non-woven mats of Ag/PVA/CS blends with different PVA to CS weight ratios and different concentrations of bacteria. At the *E. coli* concentrations of 7×10^6 and 7×10^7 CFU/ml, there were still bacteria alive in the samples of PVA/CS with PVA to CS weight ratios of 96/4 and 88/12 (Fig. 8(a)), whereas no bacteria colonies were found in the non-woven mats of Ag/PVA/CS (Fig. 8(b)). Ag nanoparticles have strong antibacterial properties because Ag nanoparticles attach to the cell walls and disturb cell-wall permeability and cellular respiration (An et al., 2009; Jin et al., 2007; Son, Youk, & Park, 2006; Wei et al., 2009). Nano-sized composite fibers provide relatively larger surface areas to contact with bacteria. This suggests why, in our study, the antibacterial activity of the non-woven mats of Ag/PVA/CS blends was more pronounced than that of the non-woven mats of PVA/CS blends.

For a better understanding of the antibacterial activity of the non-woven mats of Ag/PVA/CS blends and PVA/CS blends, the antibacterial activity kinetics for Ag/PVA/CS and PVA/CS blends toward *E. coli* was investigated; the results are shown in Fig. 8(c). It was observed that the non-woven mats of Ag/PVA/CS blends exhibited higher antibacterial activity than that of non-woven mats of PVA/CS blends. The Ag/PVA/CS could kill all the bacteria within 6 h, whereas the PVA/CS non-woven mat was bacteriostatic only at the bacteria concentration of about 7×10^6 CFU/ml. Thus, our study results indicate that the presence of Ag nanoparticle incorporation in PVA/CS nanofibers can significantly improve the antibacterial property of this material.

4. Conclusions

Non-woven mats of PVA/CS blends and PVA/CS blends containing 1 wt% Ag nanoparticles were successfully fabricated by the electrospinning method. PVA was partially miscible with CS and had good electrospinnability when blended with CS, which cannot be electrospun alone. The addition of $AgNO_3$ to the polymer blend solution of PVA and CS improved the electrospinnability of the blend. The formation of Ag nanoparticles on the surface of e-spun fibers was confirmed by obtaining TEM micrographs and by XRD. The Ag nanoparticles in the polymer showed antibacterial activity and acted as a nucleating agent during cold crystallization. The CS in the PVA/CS blend solutions resulted in a reduction in the diameter of the e-spun fibers and an increase in the tensile strength of a non-woven mat of the PVA/CS blend; however, the elongation of the mat decreased. The antibacterial experiment indicated that the non-woven mats of PVA/CS blends had good bactericidal activity against the gram-negative bacteria *E. coli*. The antibacterial activity of non-woven mats of Ag/PVA/CS blends was better than that of non-woven mats of PVA/CS blends. The addition of $AgNO_3$ to the PVA/CS blend solutions enhanced not only the electrospinning performance but also the antibacterial ability of the non-woven mats of PVA/CS.

Acknowledgment

We thank Ms. Hye-Jin Cho of the Division of Electron Microscopic Research, Korea Basic Science Institute, for her help in taking the TEM images.

References

An, J., Zhang, H., Zhang, J., Zhao, Y., & Yuan, X. (2009). Preparation and antibacterial activity of electrospun chitosan/poly(ethylene oxide) membranes containing silver nanoparticles. *Colloid and Polymer Science*, *287*, 1425–1434.

Chuanchamsai, A., Lertviriyasawat, S., & Danwanichakul, P. (2008). Spinnability & defect formation of chitosan/poly vinyl alcohol electrospun nanofibers. *Thammasat International Journal of Science and Technology*, *13*, 24–29.

Ding, B., Kim, H. Y., Lee, S. C., Lee, D. R., & Choi, K. J. (2002). Preparation and characterization of nanoscaled poly(vinyl alcohol) fibers via electrospinning. *Fibers and Polymers*, *3*, 73–79.

Giner, S. T., Ocio, J. M., & Lagaron, J. M. (2008). Development of active antimicrobial fiber based chitosan polysaccharide nanostructures using electrospinning. *Engineering in Life Sciences*, *8*, 303–314.

Giner, S. T., Ocio, M. J., & Lagaron, J. M. (2009). Novel antimicrobial ultrathin structures of zein/chitosan blends obtained by electrospinning. *Carbohydrate Polymers*, *77*, 261–266.

Hong, K. H., Park, J. L., Sul, I. H., Youk, J. H., & Kang, T. J. (2006). Preparation of antimicrobial poly(vinyl alcohol) nanofibers containing silver nanoparticles. *Polymer Physics*, *44*, 2468–2474.

Ignatova, M., Manolova, N., & Rashkov, I. (2007). Novel antibacterial fibers of quaternized chitosan and poly(vinyl pyrrolidone) prepared by electrospinning. *European Polymer Journal*, *43*, 1112–1122.

Ignatova, M., Starbova, K., Markova, N., Manolova, N., & Rashkov, I. (2006). Electrospun nano-fiber mats with antibacterial properties from quaternised chitosan and poly(vinyl alcohol). *Carbohydrate Research*, *341*, 2098–2107.

Jameela, S. R., & Jayakrishnan, A. (1995). Glutaraldehyde cross-linked chitosan microspheres as a long acting biodegradable drug delivery vehicle: Studies on the in vitro release of mitoxantrone and in vivo degradation of microspheres in rat muscle. *Biomaterial*, *16*, 769–775.

Jia, Y. T., Gong, J., Gu, X. H., Kim, H. Y., Dong, J., & Shen, X. Y. (2007). Fabrication and characterization of poly (vinyl alcohol)/chitosan blend nanofibers produced by electrospinning method. *Carbohydrate Polymers*, *67*, 403–409.

Jin, J. W., Jeon, H. J., Kim, J. H., & Youk, J. H. (2007). A study on the preparation of poly(vinyl alcohol) nanofibers containing silver nanoparticles. *Synthetic Metals*, *157*, 454–459.

Jin, Y., Yang, D. Z., Zhou, Y. Z., Ma, G., & Nie, J. (2008). Photocrosslinked electrospun chitosan-based biocompatible nanofibers. *Journal of Applied Polymer Science*, *109*, 3337–3343.

Khoo, C. G. L., Franzich, S., Rosinski, A., Sjostrom, M., & Hoogstraate, J. (2003). Oral gingival delivery systems from chitosan blends with hydrophilic polymers. *European Journal of Pharmaceutics and Biopharmaceutics*, *55*, 47–56.

Kim, S. E., Kim, H. S., & Lee, H. C. (2010). Electrospinning of polylactide fibers containing silver nanoparticles. *Macromolecular Research*, *18*, 215–221.

Muzarelli, R. A. A. (2009). Chitins and chitosan for the repair of wounded skin, nerve, cartilage and bone. *Carbohydrate Polymers*, *76*, 167–182.

Park, W. H., Leong, L., Yoo, D., & Huson, S. (2004). Effect of chitosan on morphology and conformation of electrospun silk fibroin nanofibers. *Polymer*, *45*, 7151–7157.

Park, J. S., Park, J. W., & Ruckenstein, E. (2001). Thermal and dynamic mechanical analysis of PVA/MC blend hydrogels. *Polymer*, *42*, 4271–4280.

Pillai, C. K. S., Paul, W., & Sharma, C. P. (2009). Chitin and chitosan polymer: Chemistry, solubility and fiber formation. *Progress in Polymer Science*, *34*, 641–678.

Shalumon, K. T., Biulal, N. S., Selvamurugan, N., Nair, S. V., Menon, D., Furuike, T., et al. (2009). Electrospinning of carboxymethyl chitin/poly(vinyl alcohol) nanofibrous scaffold for tissue engineering applications. *Carbohydrate Polymers*, *77*, 863–869.

Son, W. K., Youk, J. H., Lee, T. S., & Park, W. H. (2004). The effect of solution properties and polyelectrolyte on electrospinning of ultrafine poly(ethylene oxide) fibers. *Polymer*, *45*, 2959–2966.

Son, W. K., Youk, J. H., & Park, W. H. (2006). Antimicrobial cellulose acetate nanofibers containing silver nanoparticles. *Carbohydrate Polymers*, *65*, 430–434.

Velmurugan, N., Kumar, G. G., Han, S. S., Nahm, K. S., & Lee, Y. S. (2009). Synthesis and characterization of potential fungicidal silver nano-sized particles and chitosan membrane containing silver particles. *Iranian Polymer Journal*, *18*, 383–392.

Wei, D. W., Sun, W., Qian, W. P., Ye, Y. Z., & Ma, X. (2009). The synthesis of chitosan-based silver nanoparticles and their antibacterial activity. *Carbohydrate Research*, *344*, 2375–2382.

Zheng, H., Du, Y., Yu, J., Huang, R., & Zhang, L. (2001). Preparation and characterization of chitosan/poly(vinyl alcohol) blend fibers. *Journal of Applied Polymer Science*, *80*, 2558–2565.

Zhou, Y. S., Yang, D. Z., & Niel, J. (2006). Electrospinning of chitosan/poly(vinyl alcohol) acrylic acid aqueous solutions. *Journal of Applied Polymer Science*, *102*, 5692–5697.

Zong, X. H., Kim, K. S., Fang, D. F., Ran, S. F., Hsiao, B. S., & Chu, B. J. (2002). Structure and process relationship of electrospun biobsorbable nanofiber membranes. *Polymer*, *43*, 4403–4412.